Endosperm turgor pressure decreases during early Arabidopsis seed development

Léna Beauzamy[1+], Chloé Fourquin[1+], Nelly Dubrulle[1], Yann Boursiac[2], Arezki Boudaoud[1*], Gwyneth Ingram[1*]

[1] Laboratoire Reproduction et Développement des Plantes, Univ Lyon, ENS de Lyon, UCB Lyon 1, CNRS, INRA, F-69342, Lyon, France

[2] Biochimie et Physiologie Moléculaire des Plantes, Unité Mixte de Recherche 5004, CNRS/INRA/Montpellier SupAgro/Université de Montpellier, Montpellier,

[+] These authors contributed equally to the manuscript.

[*]Authors for correspondence: Gwyneth INGRAM (Gwyneth.Ingram@ens-lyon.fr), Arezki BOUDAOUD (Arezki.Boudaoud@ens-lyon.fr).

ABSTRACT

In *Arabidopsis,* rapid expansion of the coenocytic endosperm after fertilization has been proposed to drive early seed growth, which is in turn constrained by the seed coat. This hypothesis implies physical heterogeneity between the endosperm and seed coat compartments during early seed development, which to date has not been demonstrated. Here we combine tissue indentation with modelling to show that the physical properties of the developing seed are consistent with the hypothesis that elevated endosperm-derived turgor pressure drives early seed expansion. We provide evidence that whole-seed turgor is generated by the endosperm at early developmental stages. Furthermore, we show that endosperm cellularization and seed growth arrest are associated with a drop in endosperm turgor pressure. Finally we demonstrated that this decrease is perturbed when the function of POLYCOMB REPRESSIVE COMPLEX2 is lost, suggesting that turgor pressure changes could be a target of genomic imprinting. Our results indicate a developmental role for changes in endosperm turgor-pressure in the *Arabidopsis* seed.

INTRODUCTION

Differential regulation of turgor pressure is of key physiological importance in plants, a classical example being the rapid regulation of guard cell turgor during stomatal movements. During development however, although turgor pressure drives plant growth, differential growth is generally thought to be achieved by regulated changes in cell wall extensibility, rather than by changes in cell turgor pressure (Beauzamy et al., 2014). A potential exception is the developing seed. Seed development involves the co-ordinated growth of maternal seed coat tissues and the enclosed zygotic endosperm and embryo. In *Arabidopsis,* rapid expansion of the coenocytic endosperm after fertilization has been proposed to drive early seed growth, which is in turn constrained by the seed coat (Creff et al., 2015; Garcia et al., 2005; Garcia et al., 2003; Ingram, 2010). The growing seed is a major sucrose sink, and sucrose import from the testa to the endosperm plays an important role in Arabidopsis seed development (Chen et al., 2015). Evidence from several species exists to suggest that sucrose is actively converted to hexoses in the coenocytic endosperm. In oilseed rape, hexose accumulates in a separate endosperm compartment to that surrounding the developing embryo (Morley-Smith et al., 2008), and is proposed to serve a function other than embryo nutrition. In Arabidopsis, high hexose levels have also been measured in young seeds, and hexose/sucrose ratios have been shown to drop during endosperm cellularization, which occurs at around the heart stage in embryo development (Hehenberger et al., 2012). One hypothesis then, is that the vacuole of the early coenocytic endosperm accumulates very high levels of hexoses, and potentially other metabolites (such as organic acids) (Schmidt et al., 2007), in order to actively reduce its osmotic potential and drive water uptake from surrounding maternal tissues, driving swelling of the central vacuole, and thus growth.

A mechanistic understanding of the basis of early endosperm growth necessitates the application of quantitative methods to assess the relative properties of different seed compartments. The Arabidopsis endosperm is small and inaccessible, enclosed within several layers of maternally derived cells (the seed coat, formed from two integuments). This makes *in vivo* sampling techniques, (direct measurement of turgor pressure, or sampling of vacuole contents) very challenging. Conversely, the

small size and relatively simple structure of the *Arabidopsis* seed renders possible its characterisation using non-invasive measurements of whole tissue mechanical properties. With this in mind we investigated the feasibility of using tissue indentation (Beauzamy et al., 2015; Forouzesh et al., 2013; Routier-Kierzkowska and Smith, 2014) as a means of inferring the physical properties of the developing seed.

RESULTS

Early endosperm development in Arabidopsis has been extensively characterised, and involves nuclear division in the absence of cytokinesis accompanied by rapid expansion of the central vacuole of the endosperm, and rapid seed expansion. Expansion decreases dramatically when the embryo reaches the early heart stage, and the coenocytic endosperm then cellularizes progressively in a wave that initiates around the developing embryo and progresses towards the chalazal pole (Fig. 1a)(Brown et al., 2003; Brown et al., 1999; Sorensen et al., 2002)(Boisnard-Lorig et al., 2001). We concentrated our observations on early stages of seed development, starting at the early-globular stage (when the seed is actively expanding and the endosperm uncellularized), and ending at the late heart-early torpedo stage (when the endosperm has completed cellularization and started to degenerate to allow embryo growth). Seeds were removed from siliques, immobilized on adhesive tape at the base of a Petri dish, and submerged in a water film. Seed sizes for each experimental stage were extracted from confocal stacks of seeds from plants expressing an Lti6B membrane marker (Cutler et al., 2000) (Supplementary Fig. 1). Mechanical measurements were only made on undamaged seeds oriented horizontally to minimize variability. The experimental setup is shown in Fig. 1b.

Force *vs.* displacement curves were obtained for a controlled compression of 30 micrometres using a flat circular tip 100 micrometres in diameter (Fig.1c and Supplementary Fig. 2). Repeated indentations on single seeds two hours later showed that indentation did not cause damage to individual seeds (Supplementary Fig. 2b). Most force displacement curves appeared to be near-linear at maximum indentation. We deduced stiffness (k) values for seeds at maximum indentation by applying a linear fit to these curves (Fig. 2a). Repeated indentations on seeds at 2 minute intervals using different loading

rates did not significantly alter stiffness values suggesting that water movement and plastic deformation are minimal in our system; extend curves were particularly insensitive to loading rates, leading us to focus on the slope of these curves (Supplementary Fig. 2c). We found that at maximum indentation younger seeds (stages 1-4) were significantly stiffer than older seeds (stages 5 and 6) (Fig. 2b).

It has been previously shown that the slope for indentation curves can be principally attributed to turgor (Routier-Kierzkowska and Smith, 2014). As seed growth is believed to be driven by the endosperm, we tested the contribution of the endosperm to total seed stiffness by releasing endosperm turgor pressure through seed puncture using a microinjection apparatus. At early stages (1-2), seed puncture generally leads to a dramatic loss of seed stiffness (Fig. 3a). We conclude that at these stages most of stiffness of the seed derives from the turgidity of the uncellularized endosperm. To further test this idea we identified osmotic conditions permitting plasmolysis of the testa and a change in geometry of the endosperm consistent with a reduction in turgor (Supplemental Fig 3a and b). This treatment led to a dramatic decrease in seed stiffness in young seeds (Fig. 3b, Supplementary Fig. 2c). In contrast seed puncture at later stages does not lead to a significant decrease in seed stiffness, although plasmolysis leads to a significant softening (Fig. 3b, Supplementary Fig. 2c). At these later stages the endosperm is cellularized, and it is unlikely that the majority of endosperm cells are disrupted by endosperm puncture. To test whether the physical properties of the seed coat might vary during the developmental window studied we carried out 1μm indentations of seed coat cells with an Atomic Force Microscope. Under these conditions measurements are mostly influenced by cell turgor pressure (Beauzamy et al., 2014). We were unable to detect significant differences in stiffness of the outer cells of the testa between the globular and late heart stage of development (Supplementary Fig. 3c). Finally, we found the hysteresis (difference) between extend and retract curves was increased in plasmolysed seeds, suggesting that this hysteresis is mostly due to viscoelasticity of cell walls. (Supplementary Fig. 2c)

To further test whether seed stiffness can be attributed to the characteristics of the developing endosperm, we investigated the stiffness of populations of seeds from plants heterozygous for

fertilization independent seed2-5 (fis2-5) (Weinhofer et al., 2010). *FIS2* encodes an endosperm specific component of the endosperm growth-restricting POLYCOMB REPRESSIVE COMPLEX2 (PRC2). The *FIS2* gene is paternally imprinted and thus only expressed from the maternal genome during early endosperm development. Seeds inheriting a mutant maternal copy of *FIS2* in the zygotic compartment (50% of seeds in the siliques of self-fertilized *FIS2/fis2-5* heterozygotes) arrest when embryos are at the early heart stage of development (Luo et al., 2000). Arrested seeds have been reported to be larger than their siblings, and show a total lack of endosperm cellularization (Hehenberger et al., 2012)(Luo et al., 2000). Recently it was shown that arresting seeds maintain higher hexose levels than their siblings, and a convincing correlation between cellularisation and decreasing whole-seed hexose levels was established (Hehenberger et al., 2012), suggesting a potential drop in osmotic pressure at cellularization. Here we investigated whether the altered endosperm development of seeds with endosperms inheriting a maternal *fis2-5* allele might translate into a detectable difference in the mechanical properties in a segregating population. We found that in the self pollinated siliques of *FIS2/fis2-5* plants (where 50% of zygotic compartments carry a maternal *fis2-5* allele), although average seed stiffness was not significantly different to that in the siliques of *FIS2/FIS2* sibling plants at stage 2, it was significantly increased at stages 4 and 5, and significantly decreased at stage 6 (when arrested seeds have started to degenerate) (Fig. 3c). The sizes and shapes of seeds from *FIS2/FIS2* and *FIS2/fis2-5* plants were not significantly different at these developmental stages (Supplementary Fig. 4A). Since the seed coats of all the seeds of *FIS2/fis2-5* heterozygous plants are genetically identical, and *FIS2* expression is endosperm specific, we can conclude that differences in seed hardness are entirely due to differences in the physical properties of the zygotic compartment, and may underlie the increased expansion of seeds containing maternally inherited copies of *fis2-5*.

Although the stiffness values obtained from indentation reflect turgor, absolute values of turgor pressure can only be derived from stiffness by taking into account the geometry of the turgid compartment (Vella et al., 2012) (Fig. 4a). In a previous study we showed that soon after fertilization, endosperm derived pressure is perceived in an internal cell layer of the seed coat (the inner cell layer

of the outer integument), which subsequently undergoes thickening of its inner cell wall (Creff et al., 2015). We considered this cell wall to be load-bearing, and other cell walls to have small contributions to seed mechanics before the completion of cellularization. We therefore assumed that the developing seed can be approximated by a thin pressurized shell of the same geometry as the load-bearing wall (Kutschera and Niklas, 2007). We calculated values for its longitudinal and transverse curvature from confocal stacks obtained from the seeds of Lti6B:GFP-expressing lines for each of the developmental stages considered in this study (Fig. 4b,c). When indentation depths (m) are greater than shell thickness, the slope, k (N/m), of force curves is proportional to inverse mean curvature (κ_M) (m^{-1}) and to pressure (P) (N/m^2) (Vella et al., 2012) (see relationship in Fig. 4a). Accordingly, pressure values were calculated from the values of k obtained for wild type seeds (Fig. 4d) and for populations of seeds from *FIS2/FIS2* and *FIS2/fis2-5* plants (Supplementary Fig. 4B). For wild-type seeds we found that although pressure values did not differ significantly between stages 1 and 2, they decreased significantly between stages 2 and 3 and between each subsequent stage until stage 5. No significant difference in pressure was observed between stages 5 and 6. A similar trend was observed for seed populations from *FIS2/FIS2* plants (Supplementary Fig. 4C). Average pressure values decreased from a maximum of around 0.15MPa at stage 1 to around 0.06MPa at stage 6. To validate calculated pressure values we made direct pressure measurements using a classical pressure probe apparatus (Azaizeh et al., 1992). In seeds amenable to measurement (note that more than 75% of seeds give no useable reading), the range of pressure values obtained using this technique at the globular and heart stages was very similar to our calculated values (Supplementary Fig. 4b), but showed a disproportionately number of low readings, highlighting the need for alternative methodologies for measuring turgor pressure in this system.

DISCUSSION

Our results support the hypothesis that endosperm turgor pressure is elevated during early seed development, leading to a physical heterogeneity between seed tissues which could act to promote seed growth. In accordance with this idea, our measurements appear consistent with a positive correlation between seed growth rate and turgor pressure during seed development. Certain physical characteristics of the developing seed, in particular the fact that the maternal and zygotic compartments are symplastically isolated (Ingram, 2010; Stadler et al., 2005), may mean that this system is uniquely adapted for this mode of growth co-ordination. The endosperm effectively lives as an endo-parasite derived, in evolutionary terms, from the retention of the mega-gametophyte by the sporophyte. This evolutionary origin may underlie the acquisition of a mode of growth co-ordination based upon the unidirectional transfer of nutrients from the mother plant to the zygotic compartment, and the subsequent imposition of physical force by the latter on the sporophytic « host », rather than on more subtle bilateral signalling. Our observations thus indicate a convergence of developmental mechanisms in the seed, with those observed in other plant tissues, such as the stem, where the epidermis constrains growth driven by hydrostatic pressure in underlying cells (Kutschera and Niklas, 2007). In this context it is interesting to note that our results suggest that the regulation of endosperm turgor, could be target of maternal control through the activity of PRC2 in angiosperms. Differences in turgor pressure in seeds with a *fis2-5* zygotic compartment appear to precede endosperm cellularization, thus raising the question of whether a loss of turgor-pressure reduction in the endosperm could, in part, underlie of the lack of endosperm cellularization and embryo growth observed in these seeds. Whether the elevated whole-seed hexose levels observed in these seeds is a cause or, as previously suggested (Hehenberger et al., 2012), an effect of lack of cellularization is a question deserving further scrutiny.

MATERIALS AND METHODS

Plant growth conditions

Seeds were plated on Murashige and Skoog (MS) media, vernalized for 3 days at 4°C, germinated under short day conditions (8 hours light) at 18°C. Plantlets were transferred to soil in identical growth room conditions for 3 weeks and finally placed under continuous light at 16°C. To ensure synchronicity between plants, flowers were labelled and dated at anthesis.

Indenter sample preparation and settings

Following silique opening, seeds were placed individually on adhesive tape on microscope slides in water drops. Slides were placed on the extended stage of the nanoindentor (TI 950 TriboIndenter, Hysitron). A truncated cone tip with a flat end of ~100 µm diameter (nominal value = 96.96 µm) was used for indentations. The "displacement-controlled" mode was used to allow imposition of a maximum indentation of 30 µm with a specific load rate of 6 µm/s (5s extend, 5s retract). High-resolution force-displacement curves were recorded with a data acquisition rate of 200 points/s. After all indentations were complete water was removed and replaced by a drop of clearing solution ((1V glycerol / 7V chloral hydrate, liquid solution VMR CHEMICALS) to allow developmental staging. Coverslips were applied and samples were placed for 3 hours at room temperature or overnight at 4°C before visualisation under DIC optics using a ZEISS AX10.

Genotyping

The *fis2-5* allele (Weinhofer et al., 2010) (Col-0 ecotype, SALK_009910) was used in this study. Plant DNA was extracted with a rapid CTAB isolation technique(Stewart and Via, 1993). The primers *fis2genoF* (TGTTGTTTCCATGATTTCTTTTTC) and *fis2genoR* (AAACCGAACCAGTTTTCATACC) were used to isolate the WT fragment and *fis2genoR* and *SALK LB* (ATTTGCCGATTTCGGAAC) for the T-DNA insertion.

Confocal imaging

Confocal imaging was performed on a Leica SP8 up-right confocal microscope equipped with a 25x water immersion objective (HCX IRAPO L 25x/0.95 W) and one LED laser emitting at a wavelength of 488nm (Leica Microsystems, Wetzlar, Germany). Images were collected at 495-545 nm for GFP, using mosaic images for large seeds. Stitching was performed with the LAS (Leica Acquisistion System) software. The following scanning settings were used: pinhole size 1AE, 1.25x zoom, 5% laser power, scanning speed of 8000 Hz (resonant scanner), frame averaging 4 to 6 times and Z intervals of 0.5µm.

Statistical analysis

Statistical analyses were performed using R (R Development Core Team, 2012). Based on Shapiro's and Barltett's tests the data were in general neither normal nor homoscedastic, we therefore used Wilcoxon's rank-sum test (equivalent to the Mann and Whitney test), a non parametric rank-based test, to determine statistical differences.

AUTHOR CONTRIBUTIONS

C.F., L.B., N.D. and Y.B. carried out experiments, analysed results and prepared figures. All authors participated in experimental design and in manuscript preparation. G.I. and A.B. planned and directed the project.

ACKNOWLEDGEMENTS

We would like to thank Claudia Köhler (Uppsala Biocenter, Sweden) for providing *fis2* seeds and for useful discussions, Marie Delattre (CNRS, ENS de Lyon) for the use of her microinjection apparatus, and the plant culture, logistics and secretarial teams at the RDP (ENS de Lyon) for their support. This work was funded by a fellowship from AgreenSkills (CESETAB project) and INRA awarded to CF, a "Chaire d'excellence" (ANR-10-CHEX-0011: mécanograine) from l'Agence Nationale de la Recherche, France awarded to GI, and a European Research Council Starting Grant (Phymorph #307387) awarded to AB.

REFERENCES

Azaizeh, H., Gunse, B. and Steudle, E. (1992). Effects of NaCl and CaCl(2) on Water Transport across Root Cells of Maize (Zea mays L.) Seedlings. *Plant Physiol* **99**, 886-894.

Beauzamy, L., Derr, J. and Boudaoud, A. (2015). Quantifying hydrostatic pressure in plant cells by using indentation with an atomic force microscope. *Biophys J* **108**, 2448-2456.

Beauzamy, L., Nakayama, N. and Boudaoud, A. (2014). Flowers under pressure: ins and outs of turgor regulation in development. *Annals of botany* **114**, 1517-1533.

Boisnard-Lorig, C., Colon-Carmona, A., Bauch, M., Hodge, S., Doerner, P., Bancharel, E., Dumas, C., Haseloff, J. and Berger, F. (2001). Dynamic analyses of the expression of the HISTONE::YFP fusion protein in arabidopsis show that syncytial endosperm is divided in mitotic domains. *Plant Cell* **13**, 495-509.

Brown, R. C., Lemmon, B. E. and Nguyen, H. (2003). Events during the first four rounds of mitosis establish three developmental domains in the syncytial endosperm of Arabidopsis thaliana. *Protoplasma* **222**, 167-174.

Brown, R. C., Lemmon, B. E., Nguyen, H. and Olsen, O. A. (1999). Development of endosperm in Arabidopsis thaliana. *Sexual Plant Reproduction* **12**, 32-42.

Chen, L. Q., Lin, I. W., Qu, X. Q., Sosso, D., McFarlane, H. E., Londono, A., Samuels, A. L. and Frommer, W. B. (2015). A cascade of sequentially expressed sucrose transporters in the seed coat and endosperm provides nutrition for the Arabidopsis embryo. *Plant Cell* **27**, 607-619.

Creff, A., Brocard, L. and Ingram, G. (2015). A mechanically sensitive cell layer regulates the physical properties of the Arabidopsis seed coat. *Nat Commun* **6**, 6382.

Cutler, S. R., Ehrhardt, D. W., Griffitts, J. S. and Somerville, C. R. (2000). Random GFP::cDNA fusions enable visualization of subcellular structures in cells of Arabidopsis at a high frequency. *Proc Natl Acad Sci U S A* **97**, 3718-3723.

Forouzesh, E., Goel, A., Mackenzie, S. A. and Turner, J. A. (2013). In vivo extraction of Arabidopsis cell turgor pressure using nanoindentation in conjunction with finite element modeling. *Plant J* **73**, 509-520.

Garcia, D., Fitz Gerald, J. N. and Berger, F. (2005). Maternal control of integument cell elongation and zygotic control of endosperm growth are coordinated to determine seed size in Arabidopsis. *Plant Cell* **17**, 52-60.

Garcia, D., Saingery, V., Chambrier, P., Mayer, U., Jurgens, G. and Berger, F. (2003). Arabidopsis haiku mutants reveal new controls of seed size by endosperm. *Plant Physiol* **131**, 1661-1670.

Hehenberger, E., Kradolfer, D. and Kohler, C. (2012). Endosperm cellularization defines an important developmental transition for embryo development. *Development* **139**, 2031-2039.

Ingram, G. C. (2010). Family life at close quarters: communication and constraint in angiosperm seed development. *Protoplasma* **247**, 195-214.

Kutschera, U. and Niklas, K. J. (2007). The epidermal-growth-control theory of stem elongation: an old and a new perspective. *J Plant Physiol* **164**, 1395-1409.

Luo, M., Bilodeau, P., Dennis, E. S., Peacock, W. J. and Chaudhury, A. (2000). Expression and parent-of-origin effects for FIS2, MEA, and FIE in the endosperm and embryo of developing Arabidopsis seeds. *Proc Natl Acad Sci U S A* **97**, 10637-10642.

Morley-Smith, E. R., Pike, M. J., Findlay, K., Kockenberger, W., Hill, L. M., Smith, A. M. and Rawsthorne, S. (2008). The transport of sugars to developing embryos is not via the bulk endosperm in oilseed rape seeds. *Plant Physiol* **147**, 2121-2130.

Routier-Kierzkowska, A. L. and Smith, R. S. (2014). Mechanical measurements on living plant cells by micro-indentation with cellular force microscopy. *Methods Mol Biol* **1080**, 135-146.

Schmidt, R., Stransky, H. and Koch, W. (2007). The amino acid permease AAP8 is important for early seed development in Arabidopsis thaliana. *Planta* **226**, 805-813.

Sorensen, M. B., Mayer, U., Lukowitz, W., Robert, H., Chambrier, P., Jurgens, G., Somerville, C., Lepiniec, L. and Berger, F. (2002). Cellularisation in the endosperm of Arabidopsis thaliana is coupled to mitosis and shares multiple components with cytokinesis. *Development* **129**, 5567-5576.

Stadler, R., Lauterbach, C. and Sauer, N. (2005). Cell-to-cell movement of green fluorescent protein reveals post-phloem transport in the outer integument and identifies symplastic domains in Arabidopsis seeds and embryos. *Plant Physiol* **139**, 701-712.

Stewart, C. N., Jr. and Via, L. E. (1993). A rapid CTAB DNA isolation technique useful for RAPD fingerprinting and other PCR applications. *Biotechniques* **14**, 748-750.

Vella, D., Ajdari, A., Vaziri, A. and Boudaoud, A. (2012). Indentation of ellipsoidal and cylindrical elastic shells. *Phys Rev Lett* **109**, 144302.

Weinhofer, I., Hehenberger, E., Roszak, P., Hennig, L. and Kohler, C. (2010). H3K27me3 profiling of the endosperm implies exclusion of polycomb group protein targeting by DNA methylation. *PLoS Genet* **6**.

Figures

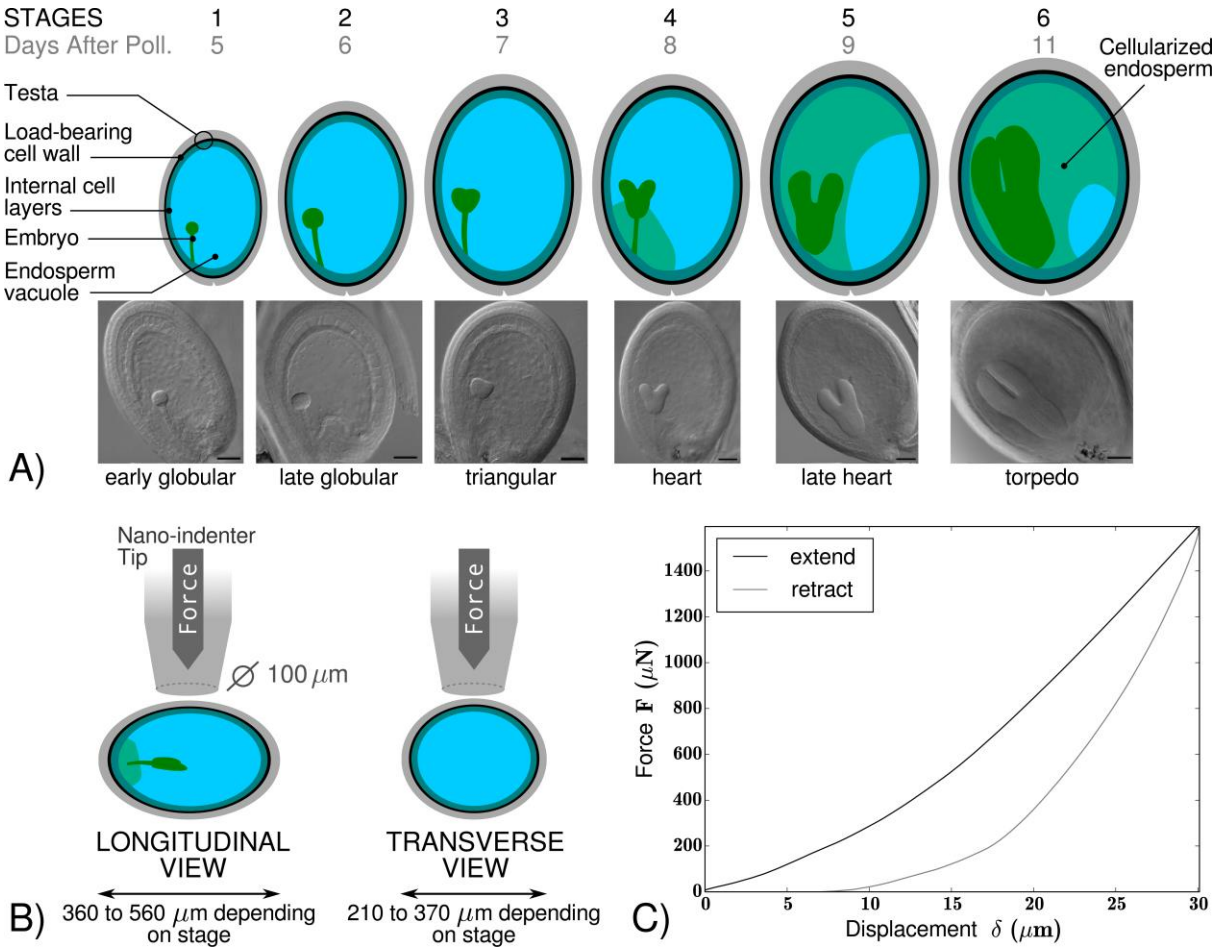

Figure 1 – Experimental system. a) Schematic diagrams of the seed developmental stages used in this study (and the corresponding timing in days after pollination) with representative images of cleared seeds from each stage. b) Schematic diagram of seed indentation setup. Seed sizes are taken from data in Supplementary Fig. 1 c) A typical curve showing force vs. displacement imposed with indenter obtained for a stage 4 seed. Further curves are provided in Supplementary Fig. 2.

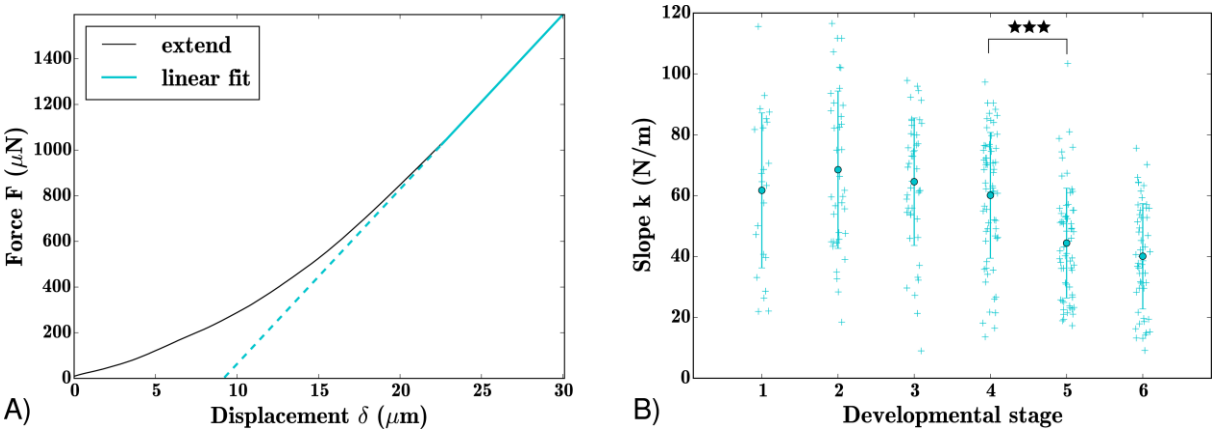

Figure 2 - Seed stiffness decreases with developmental stage. a) Typical force curve exported from indenter, with linear fit at maximum (75-100%) displacement. b) Stiffness values extracted from force v.s displacement curves at all stages of seed development. Differences between populations were evaluated statistically using a Wilcoxon rank-sum test. ***=p<0.001. Error bars indicate standard deviation around the arithmetic mean.

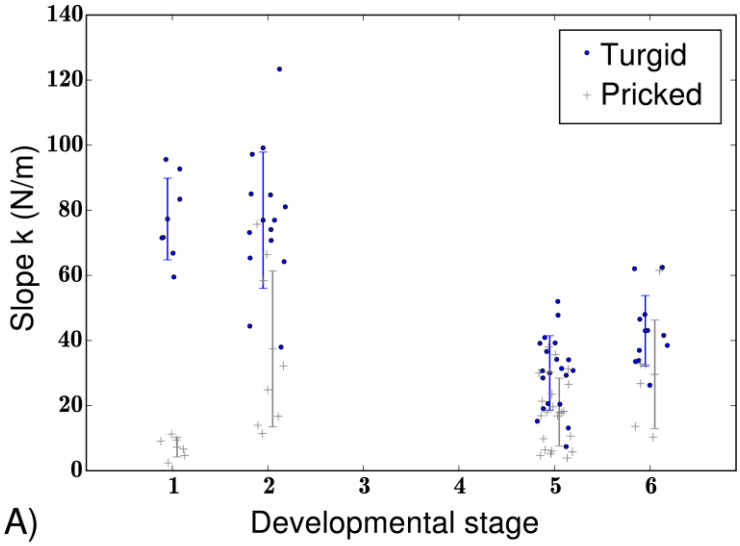
Turgid
Pricked
Slope k (N/m)
Developmental stage

A)

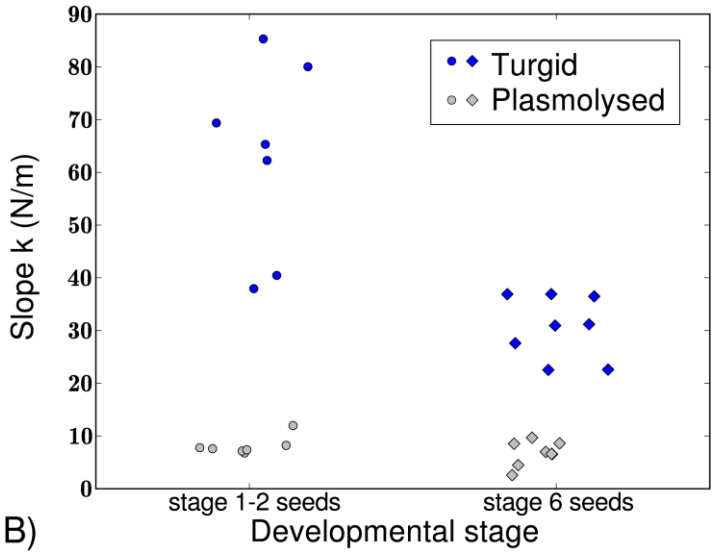
Turgid
Plasmolysed
Slope k (N/m)
stage 1-2 seeds
stage 6 seeds
Developmental stage

B)

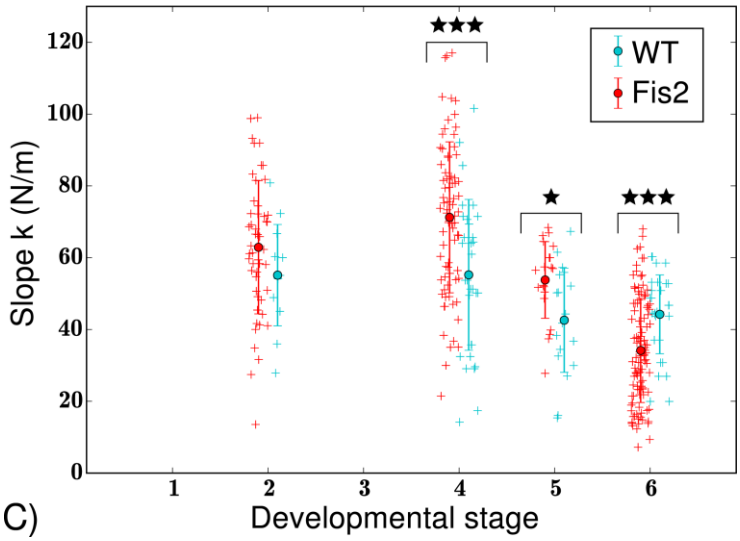
WT
Fis2
Slope k (N/m)
Developmental stage

C)

Figure 3 – Seed stiffness is mainly imposed by the endosperm at early developmental stages. a) Comparison of the stiffness of punctured seeds and intact seeds within populations at different developmental stages. Seeds were punctured laterally using an Eppendorf Femtojet microinjection and micromanipulation apparatus equipped with snapped Femtotips II injecting needles. b) Effects of osmotic treatment (0.7M mannitol for 90 minutes) on seed stiffness. c) Comparison of seed stiffness between populations of seeds from FIS2/FIS2 and FIS2/fis2-5 plants at different developmental stages. Differences between populations were evaluated statistically using a Wilcoxon rank-sum test. *=$p<0.05$, ***=$p<0.001$. Error bars indicate standard deviation around the arithmetic mean.

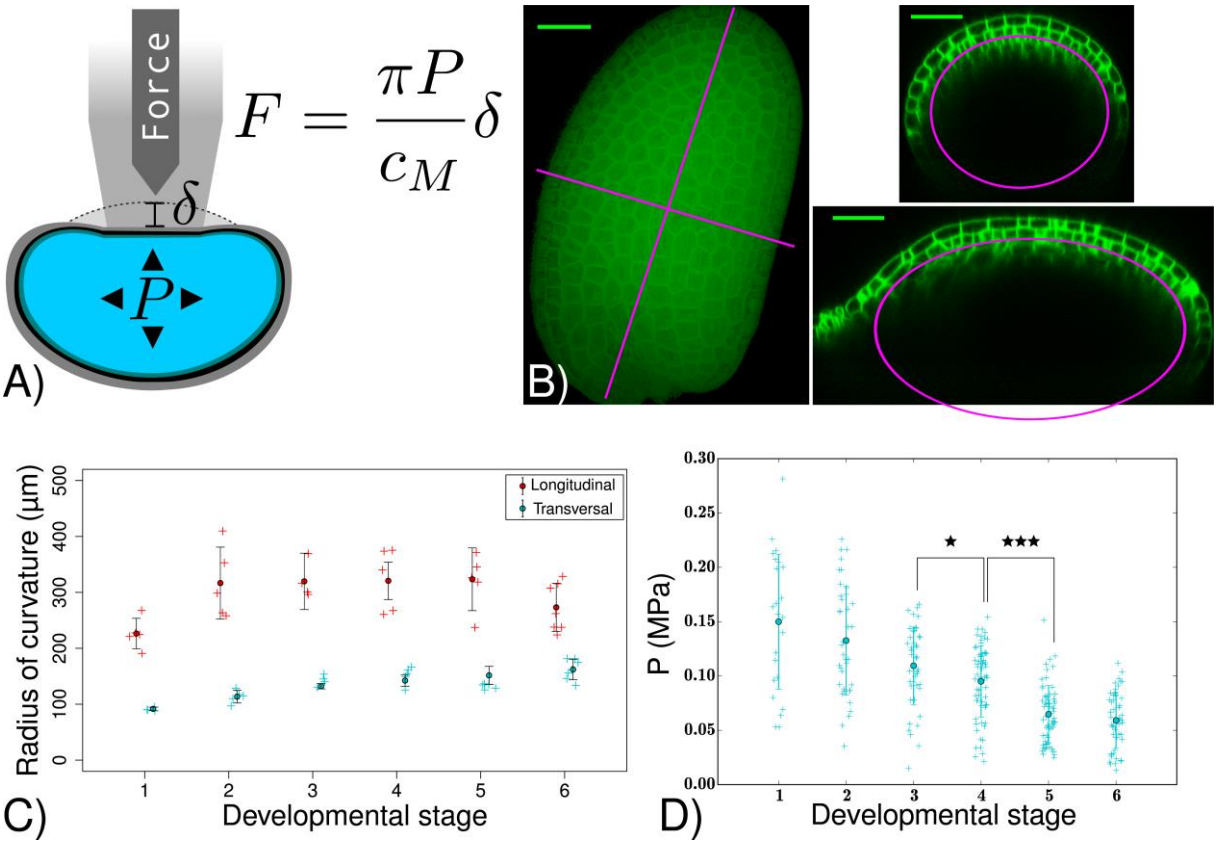

Figure 4 – Whole-seed turgor decreases during seed development. a) Parameters and equation used for pressure calculations (F=force, P=pressure, □=displacement, □$_M$=mean curvature of load-bearing cell wall) b) Representative confocal images used for extraction of curvature values. Scale bars represent 50µm. Orthogonal sections were generated using the reslice tool and an ellipse was drawn to best fit the surface of the turgid compartment of the seed. The radius curvature was then calculated using Rc = (major axe radius)² / (minor axe radius). c) Curvature values extracted from confocal stacks at different stages of wild-type seed development using Image J. d) Pressure values calculated during wild-type seed development. Differences between populations were evaluated statistically using a Wilcoxon rank-sum test. *=p<0.05, ***=p<0.001. Error bars indicate standard deviation around the arithmetic mean.